# Force Characterization of Dielectrophoresis in Droplet Transport

**Patrick M. Young and Kamran Mohseni**

*Department of Aerospace Engineering Sciences, University of Colorado at Boulder, Boulder, Colorado, USA*

**Transporting microdroplets using electric fields can be accomplished with several mechanisms, the primary methods being dielectrophoresis (DEP) for electrically insulating liquids, and electrowetting on dielectric for conducting fluids. In both cases, an electric field is applied near the leading edge of the droplet using patterned electrodes, giving rise to an electrostatic pressure that induces droplet transport. This paper examines the nature of the force distribution for DEP-actuated droplets in several electrode configurations, calculated using a numerical method designed for handling jump conditions in the Poisson equation. The numerical method is described and verified by comparison with known analytical results. The net force acting upon a DEP droplet is investigated, with the effect of electrode configuration presented for several cases, demonstrating some beneficial aspects for engineering applications.**

*Key words:* **dielectrophoresis; DEP; electrophoresis; droplet transport**

## Introduction

Digital microfluidics is a rapidly growing field, with many new and innovative applications currently being researched. Examples include variable focus lenses, display technology, fiber-optics, and lab-on-a-chip devices.[1–7] In particular, efficient and cost-effective lab-on-a-chip devices are in great demand, as they allow highly repetitive laboratory tasks to become automated with the introduction of miniaturized and integrated systems.[8] In our group, digital microfluidics has been employed for active thermal management of compact electronic devices,[9–11] design of a zero-leakage microvalve,[12] investigation of droplet morphology under electrowetting on dielectric (EWOD) actuation,[13] and design of an electrowetting microlens.[14]

Two of the most promising actuation methods of droplets for application in digital microfluidics are EWOD for conductive droplets[15–17] and dielectrophoresis (DEP) for electrically insulating droplets.[18–22] Both these methods work in a similar way: an electric field is applied near the edge of the droplet giving rise to an electrostatic pressure that induces transport. The electric field is swept down the channel, allowing for highly controlled movement of the drop.

The primary difference between an EWOD- and DEP-actuated droplet is the nature of the fluid and its effect on the electric field penetration into the media. For EWOD, an electrically conducting droplet is placed in a dielectric-coated channel lined with electrodes. A given electrode is then activated, creating an electric field that induces a charge accumulation on the surface of the fluid. This charge accumulation allows the creation of a net force upon the droplet, drawing the droplet toward the actuated electrode. DEP differs from this action in that the liquid is insulating, charge does not accumulate on the surface, and the electric field penetrates into the liquid. It is well known that a dielectric material is drawn into the gap

Address for correspondence: Kamran Mohseni, Room ECAE 175, University of Colorado, Boulder, CO 80309-0429. Voice: +303 492 0286; fax: +303 492 7881. mohseni@colorado.edu

Interdisciplinary Transport Phenomena: Ann. N.Y. Acad. Sci. 1161: 463–471 (2009).
doi: 10.1111/j.1749-6632.2008.04065.x 

between the parallel plate of a charged capacitor.[23] This is a result of the nonuniform fringing field located at the edge of the capacitor, providing a force pointing toward its center.[23,24] As opposed to EWOD, the dielectrophoretic force can act over the droplet's front face or within the bulk of the fluid itself. Jones *et al.*[20,21] have explored the close relationship between DEP and EWOD, but for direct simulation of EWOD and DEP flows including electrostatic effects, a clear description of the force distribution is required. The case considered here is for a perfect insulator (DEP), but many fluids exist that exhibit properties of both a conductor and dielectric, namely leaky dielectrics.[25]

Direct numerical simulation[26] and numerical simulations using approximations of the electrostatic effect[13,27] in droplet morphology and dynamics under EWOD and DEP have been investigated previously. Investigations into the nature of forcing in EWOD [28] and into the forcing nature of DEP have also been accomplished.[29] The focus of this paper is to extend the work of Ref. 29 using a different numerical technique, as well as presenting several different electrode configurations for application in DEP droplet transport.

## Governing Equations

The equations governing the flow of a droplet under electric effects are the mass, momentum, and electrostatic equations. Electrostatic forces can arise from free charge interactions as well as from polarization effects. In the problems considered in this investigation, the focus is droplet flow resulting from electrical forces. In most microfluidic applications the dynamic currents are so small that the magnetic field can be ignored. In this situation the governing equations for the electrical field are the electrostatic laws. For the electrostatic approximation to apply, the characteristic time scale for electric phenomena, $\tau = \epsilon/\sigma$, must be small. Note that $\tau$ is the ratio of dielectric permeability to conductivity of the medium. For the microfluidic applications considered here, this condition will usually be valid.

Consider a two-dimensional computational domain $\Omega$ and define the lower dimensional droplet interface as $\Gamma$, which divides $\Omega$ into two disjoint regions, $\Omega^-$ representing the droplet and $\Omega^+$ representing the exterior fluid. To calculate the net force acting upon the droplet, the electric potential $V(\mathbf{x})$ must be found by solving the Poisson equation

$$\nabla \cdot (\epsilon(\mathbf{x}) \nabla V(\mathbf{x})) = 0, \tag{1}$$

where $\mathbf{x} = (x, y)$ are the spatial coordinates, $\nabla = (\frac{\partial}{\partial x}, \frac{\partial}{\partial y})$, is the gradient operator, and $\epsilon(\mathbf{x})$ is the electrical permitivity of the fluid in each region. Hence, $\epsilon$ $(x)$ is constant on $\Omega^+$ and $\Omega^-$ but experiences a jump discontinuity along $\Gamma$. This jump condition can be specified as

$$[\epsilon V_n]_\Gamma = 0, \quad x \in \Gamma,$$

where

$$[\epsilon V_n]_\Gamma = \epsilon^+(\mathbf{x}) V_n^+(\mathbf{x}) - \epsilon^-(\mathbf{x}) V_n^-(\mathbf{x}). \tag{2}$$

The superscripts + and – refer to the associated variables in the regions $\Omega^\pm$, and $V_n = \nabla V \cdot \mathbf{N}$ is the normal derivative of $V$ with $\mathbf{N}$ the unit normal to the interface.

Once the electric potential has been calculated, the electric field $\mathbf{E}$ can be found using the relationship $\mathbf{E} = -\nabla V$. The net effect of an applied electrical field on a given fluid is represented by an extra body force on the right hand side of the Navier–Stokes equations. The body force density $\mathbf{f_b}$ in a fluid resulting from the influence of an electric field can be written as

$$\mathbf{f_b} = \rho_f \mathbf{E} - \frac{1}{2} E^2 \nabla \epsilon + \nabla \left( \frac{1}{2} \mathbf{E} \cdot \mathbf{E} \frac{\partial \epsilon}{\partial \rho} \right), \tag{3}$$

where $\rho$ is the density of the fluid, $\rho_f$ is the free electric charge density, and $\mathbf{E}$ is the electric field. This is the Korteweg–Helmholtz electric force density formulation.[30–32] The last term in this equation, the electrostriction force density term, can be ignored for incompressible flows

and so the body force density considered here is given by

$$\mathbf{f_b} = \rho_f \mathbf{E} - \frac{1}{2}E^2\nabla\epsilon. \tag{4}$$

This force density provides a coupling between the droplet hydrodynamics and electric field. The first term of Eq. (4) is attributed to free charge in the system, while the second term is the contribution from the polarization of the medium.

Throughout this paper, DEP forces are considered only to arise from polarization effects, and so no free charge is present. There is some discrepancy in how to represent the DEP force, but with care consistency can be achieved.[33] In contrast to the Korteweg–Helmholtz force density, the Kelvin force density is given by[34]

$$\begin{aligned}\mathbf{f_b} &= (\mathbf{P}\cdot\nabla)\mathbf{E} = ((\epsilon-\epsilon_0)\mathbf{E}\cdot\nabla)\mathbf{E}\\ &= \epsilon\nabla\left(\frac{1}{2}E^2\right) - \nabla\left(\frac{\epsilon_0}{2}E^2\right).\end{aligned} \tag{5}$$

Using the vector identity $\nabla(\phi\,\psi) = \phi\,\nabla\,\psi + \psi\,\nabla\,\phi$, we can write the Korteweg–Helmholtz force density as

$$\mathbf{f_b} = \epsilon\nabla\left(\frac{1}{2}E^2\right) - \nabla\left(\frac{\epsilon}{2}E^2\right). \tag{6}$$

For an incompressible fluid, the scalar pressure only appears in the Navier–Stokes equations in terms of a gradient. The role of pressure is to ensure that continuity of the vector field is satisfied, and the pressure takes on whatever value is needed to guarantee this condition is always fulfilled. Therefore, any other term that appears in the Navier–Stokes equations as the gradient of a scalar can be absorbed into the pressure.[34] This is true of the last term in Eqs. (5) and (6), and so the effective body force density is

$$\mathbf{f_b} = \epsilon\nabla\left(\frac{1}{2}E^2\right). \tag{7}$$

For the numerical force calculations in this paper, Eq. (7) is used to determine the force acting upon the droplet.

## Lumped Force Calculations

The *total* force, per unit area, experienced by a DEP droplet can be directly derived from capacitive energy considerations.[23,24] Differentiation of the system energy $U$ gives the net force $F$ in the horizontal direction, per unit area,

$$F = \frac{dU}{dx}.$$

This allows for the derivation of the net force acting upon a droplet in certain configurations. However, to calculate force *distributions*, numerical methods must be utilized, and this is presented in the next section.

Let $\epsilon^-$ and $\epsilon^+$ be the dielectric constant of the droplet and the external fluid, respectively. Consider the system in Figure 1, and let $x$ be the distance the droplet has extended under the charged electrode. The energy stored in the region under the charged electrode where the droplet is present is given by $\frac{1}{2}c^-V^2$, where $c^- = \frac{\epsilon^-}{H}x$ is the capacitance, per unit area, of this region. The energy stored in the region under the charged electrode where the droplet is not present is given by $\frac{1}{2}c^+V^2$, where $c^+ = \frac{\epsilon^+}{H}(L_e - x)$ is the capacitance, per unit area, of this second region. Then the net force, per unit area, is given by

$$\begin{aligned}F &= \frac{dU}{dx} = \frac{d}{dx}\left(\frac{1}{2}c^-V^2 + \frac{1}{2}c^+V^2\right)\\ &= \frac{1}{2}\frac{\epsilon^- - \epsilon^+}{H}V^2.\end{aligned} \tag{8}$$

This force is seen to be the difference in capacitive energy between a dielectric-filled channel and an empty channel. This model is only valid when the droplet interfaces are well removed from any fringing fields, where the energy argument is valid. Note that the droplet height, $H$, appears directly in this expression for $F$; this factor gives DEP a different scaling than EWOD.[35,36] The velocity of an EWOD droplet depends on $H/L$, where $L$ is the length of the droplet. In contrast, the velocity of a dielectric droplet depends only on $1/L$, making DEP

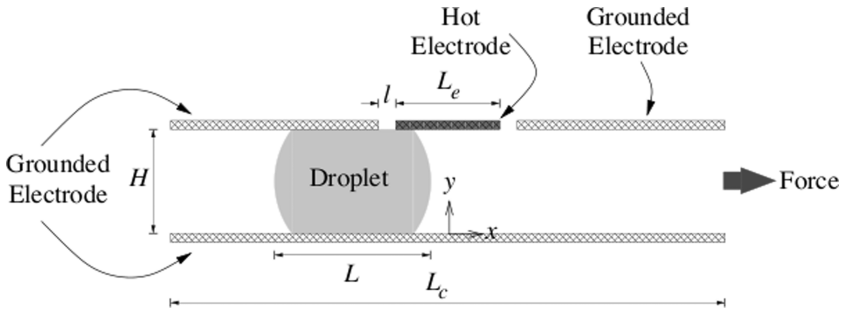


**Figure 1.** Geometry of the computational domain used in the numerical calculations. (In color in *Annals* online.)

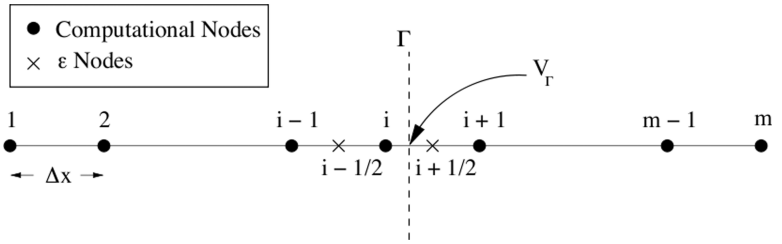


**Figure 2.** Domain used in the solution to the one-dimensional Poisson equation.

increasingly effective for very small channel sizes.

## Numerical Method

The numerical method used is a special case of the method in Ref. 37.

### Poisson Equation in One Dimension

Consider the one-dimensional version of Eq. (1), $(\epsilon V_x)_x = 0$, where $x \in [a,b]$ for simplicity. Dirichlet conditions are specified at the end points. The interface location is defined by the zero of a level set function (a signed distance function is used), $\phi(x)$. $\phi < 0$ represents the region $\Omega^-$, and $\phi > 0$ defines $\Omega^+$.

The domain is discretized by a distance $\Delta x$, see Figure 2. The solution is computed at the integer node locations. The half integer node locations are used to define the appropriate value of $\epsilon(\mathbf{x})$, determined from the average value of $\phi$ at the neighboring integer node locations. In other words if $\frac{1}{2}(\phi_{i+1} + \phi_i) \leq 0$, then $\epsilon_{i+1/2} = \epsilon^-$ and vise versa.

Away from the interface, the standard second-order centered difference can by used,

$$\left[\epsilon_{i+1/2}\left(\frac{V_{i+1} - V_i}{\Delta x}\right) - \epsilon_{i-1/2}\left(\frac{V_i - V_{i+1}}{\Delta x}\right)\right] 1/\Delta x = 0. \quad (9)$$

Special attention is required for points neighboring the interface. Define

$$\theta = \frac{|\phi_i|}{|\phi_{i+1}| + |\phi_i|},$$

and let $V_\Gamma$ represent a fictitious point on the boundary. Discretizing Eq. (2) at the boundary condition at $V_\Gamma$ gives

$$\epsilon^+ \frac{V_{i+1} - V_\Gamma}{(1-\theta)\Delta x} - \epsilon^- \frac{V_\Gamma - V_i}{\theta \Delta x} = 0. \quad (10)$$

Solving for $V_\Gamma$ using Eq. (10) yields

$$V_\Gamma = \frac{\theta\epsilon^+ V_{i+1} + (1-\theta)\epsilon^- V_i}{\theta\epsilon^+ + (1-\theta)\epsilon^-}. \quad (11)$$

The derivative to the left of the interface can now be approximated using Eq. (11),

$$\epsilon \frac{\partial V}{\partial x} \approx \epsilon^{-} \frac{V_\Gamma - V_i}{\theta \Delta x} = \hat{\epsilon} \frac{V_{i+1} - V_i}{\Delta x},$$

where

$$\hat{\epsilon} = \frac{\epsilon^{-}\epsilon^{+}}{\theta\epsilon^{+} + (1-\theta)\epsilon^{-}}.$$

The finite difference formula for $V_i$ bordering the interface to the left can therefore be written as

$$\left[\hat{\epsilon}_i \left(\frac{V_{i+1} - V_i}{\Delta x}\right) - \epsilon_{i-1/2} \left(\frac{V_i - V_{i-1}}{\Delta x}\right)\right] 1/\Delta x = 0. \quad (12)$$

Analogously, the finite difference formula for $V_{i+1}$ bordering the interface to the right is given by

$$\left[\epsilon_{i+3/2} \left(\frac{V_{i+2} - V_{i+1}}{\Delta x}\right) - \hat{\epsilon} \left(\frac{V_{i+1} - V_i}{\Delta x}\right)\right] 1/\Delta x = 0. \quad (13)$$

## Poisson Equation in Two Dimensions

Now consider Poisson's equation given by Eq. (1) in two dimensions with Dirichlet boundary conditions on the boundary and with interfacial boundary conditions given by Eq. (2). The treatment of the interface is very similar to that of the one-dimensional case, but with the added complexity of a condition on the normal derivative. Recall that the normal derivative is given by

$$V_n = \nabla V \cdot \mathbf{N} = V_x n_1 + V_y n_2, \quad (14)$$

and that the tangential derivative is

$$V_t = \nabla V \cdot \mathbf{T} = V_x n_2 - V_y n_1, \quad (15)$$

where $\mathrm{N} = (n_1, n_2)$ and $\mathrm{T} = (n_2, -n_1)$ are the unit normal and tangent, respectively. Applying Eqs. (14) and (15) to Eq. (2) gives

$$[\epsilon V_n]_\Gamma = [\epsilon V_x]_\Gamma n_1 + [\epsilon V_y]_\Gamma n_2 \quad (16)$$

$$[\epsilon V_t]_\Gamma = [\epsilon V_x]_\Gamma n_2 - [\epsilon V_y]_\Gamma n_1, \quad (17)$$

which translates to

$$[\epsilon V_x]_\Gamma = [\epsilon V_n]_\Gamma n_1 + [\epsilon V_t]_\Gamma n_2$$

$$[\epsilon V_y]_\Gamma = [\epsilon V_n]_\Gamma n_2 - [\epsilon V_t]_\Gamma n_1.$$

If it is assumed that

$$[\epsilon V_x]_\Gamma = [\epsilon V_n]_\Gamma n_1 \quad (18)$$

$$[\epsilon V_y]_\Gamma = [\epsilon V_n]_\Gamma n_2, \quad (19)$$

then Eq. (16) is satisfied exactly, while Eq. (17) gives $[\epsilon V_t]_\Gamma = 0$, which is the appropriate condition on the tangential derivative in electrostatics. Hence, the one-dimensional case can easily be extended to two dimensions, since Eqs. (18) and (19) allow the boundary condition given by Eq. (2) to be written as two separate conditions, $[\epsilon V_x]_\Gamma = [\epsilon V_y]_\Gamma = 0$. Essentially, each dimension can be considered independent of the other, allowing for simple discretization of the problem.

## Test Cases

The one-dimensional Poisson equation with jumps in $\epsilon$ at the interface can be solved analytically. Consider the problem

$$(\epsilon V_x)_x = 0, \quad V(0) = 0, \quad V(1) = 1,$$

$$\epsilon = \begin{cases} 3 \text{ if } x \le \dfrac{1}{2} \\ 1 \text{ if } x > \dfrac{1}{2} \end{cases},$$

$$\epsilon^{-} \frac{\partial V}{\partial x} = \epsilon^{+} \frac{\partial V}{\partial x} \quad \text{at} \quad x = \frac{1}{2}.$$

The exact solution is given by

$$V(x) = \begin{cases} \dfrac{1}{2}x, & x \le \dfrac{1}{2} \\ \dfrac{3}{2}x - \dfrac{1}{2}, & x > \dfrac{1}{2}. \end{cases}$$

The method captures the interfacial jump condition to machine precision as seen in Figure 3. Furthermore, there is no smearing of the jump in coefficients; it transitions precisely. In contrast, if we simply discretize over the interface

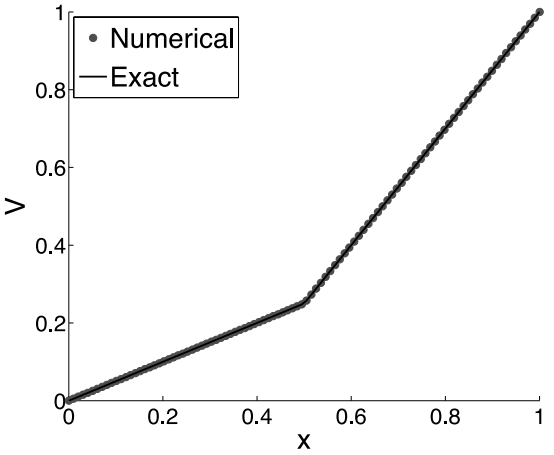


**Figure 3.** One-dimensional test case with the numerical and exact solutions plotted. (In color in *Annals* online.)

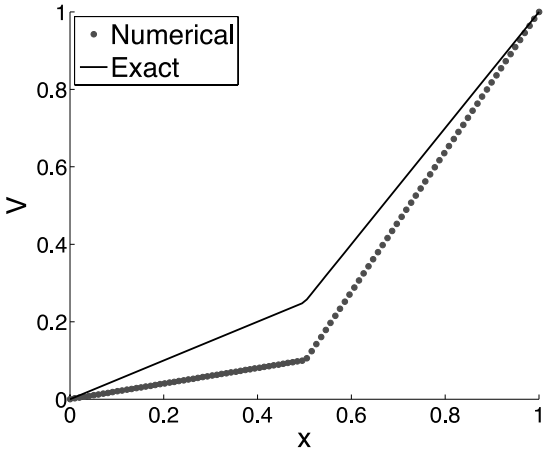


**Figure 4.** One-dimensional test case with the numerical and exact solutions plotted using a naive discretization. (In color in *Annals* online.)

as we would in the rest of the domain, the solution is incorrect, as seen in Figure 4.

A ubiquitous problem in electrostatics is that of a sphere of dielectric material placed in an otherwise uniform electric field. It is well known that the potential inside the dielectric material varies linearly with the direction of the electric field. In Figure 5, a square domain is used with Dirichlet boundary conditions applied such that a uniform field exists where there is no dielectric material present. A numerical calculation of this setup can be see in Figure 6.

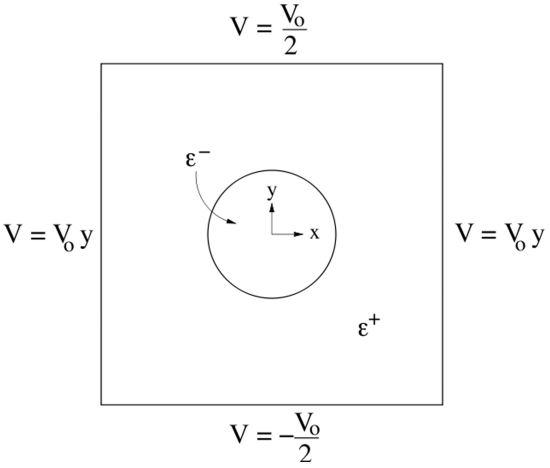


**Figure 5.** Domain used in the solution to the two-dimensional Poisson's equation test problem. The given Dirichlet conditions are specified at the boundary.

In Figure 7, the solution to Eq. (1) with $\epsilon^- = 2$ and $\epsilon^+ = 1$ has been computed using the boundary conditions specified in Figure 5. Clearly, the potential field varies linearly inside the dielectric material, as theory predicts.

## Applications

The use of DEP in microfluidics usually involves a droplet placed upon a substrate. Underlying electrodes are then activated in series giving rise to electric forces that transport the droplet to the desired location. Figure 1 shows the computational domain used to simulate DEP. The values used, unless otherwise specified, are $\epsilon^- = 3$, $\epsilon^+ = 1$, $H = 1$, $L_c = 10$, $L = 2$, $L_e = 2$, and $l = 0.05$.

Using this basic setup, the net force acting upon the droplet can be calculated by finding the electric potential and the associated electric field, and then integrating Eq. (7) along the entire channel (including the external fluid, as it also experiences electric forces). This basic DEP setup has been explored in detail previously by the authors.[29]

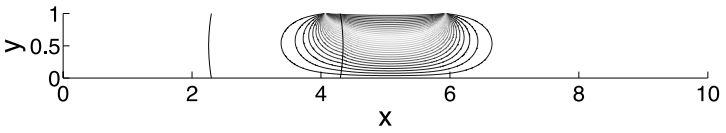


**Figure 6.** Example electric potential calculation with the electrodes only on the top of the channel. (In color in *Annals* online.)

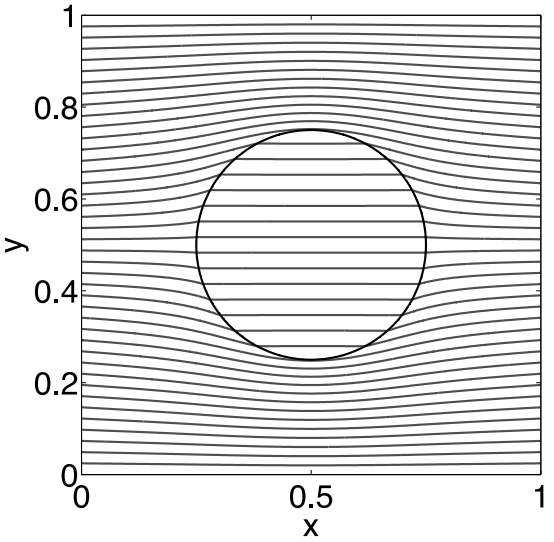


**Figure 7.** Two-dimensional test case with the numerical and exact solutions shown. (In color in *Annals* online.)

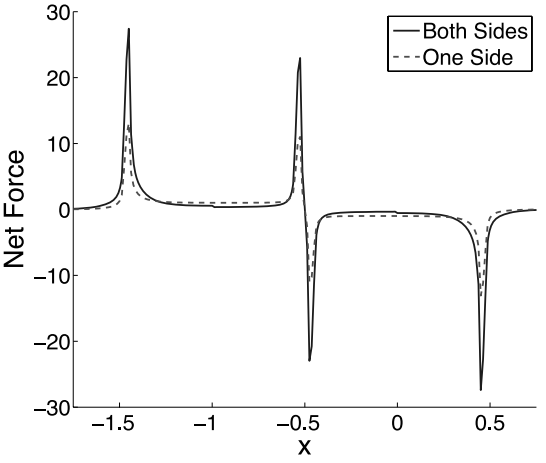


**Figure 9.** Net force experienced by a droplet with electrodes on both sides of the channel. (In color in *Annals* online.)

An alternative setup for DEP would be having patterned electrodes on both sides of the channel. Figure 8 shows an example of an electric potential calculation in such a setup, and Figure 9 compares such a setup to that of a single electrode. The net force peak experienced by the droplet is roughly twice that of a single electrode. However, the net force of the droplet in the double electrode setup when the droplet is straddled underneath the electrode, and with the droplet edges well away from the electrode edges, tends to zero. Such a setup may be useful if a strong forcing impulse is desired.

In a practical device, a droplet needs to be transported farther than one electrode width. This is done by activating electrodes in series as the droplet moves along the channel. Figure 10 shows the net force experienced by a droplet in such a configuration. As the droplet moves near the edge of a new electrode, that electrode is activated. To increase the net force experienced by a droplet while it is moving, thinner electrodes would need to be used to ensure that the next electrode was active while the droplet

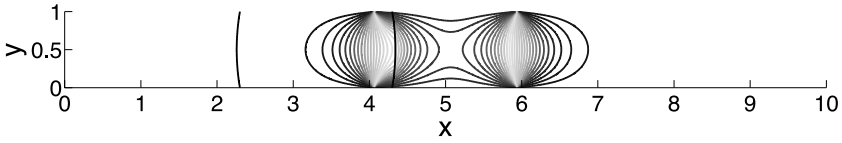


**Figure 8.** Example electric potential calculation with the electrodes on both the top and bottom of the channel. (In color in *Annals* online.)

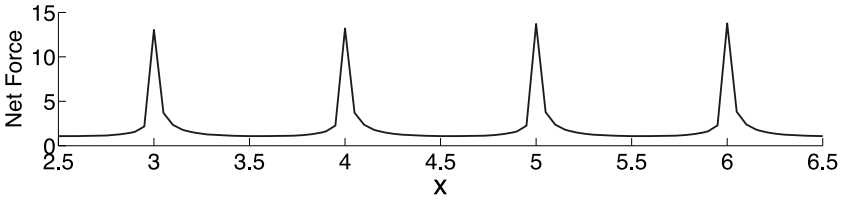


**Figure 10.** Net force experienced by a droplet from electrodes activated in series as the droplet moves through the channel. (In color in *Annals* online.)

was still under the influence of the peak in net force.

## Conclusions

In this paper, DEP, a method for droplet transport in digital microfluidics for an insulating fluid has been investigated. Droplet transport is achieved by sweeping a voltage along a microchannel ahead of the droplet. A review of the Korteweg–Helmholtz and Kelvin force density formulations has been given as well as how these force densities apply to DEP.

Investigation of the force distribution in DEP shows how the force density is spread throughout the bulk. A numerical method was demonstrated for numerically calculating the force distribution for DEP. When a droplet is under DEP actuation, small electrode sizes in comparison to droplet length are preferable, as they keep the net force pointing in the same direction as the droplet moves under the electrode, avoiding any possible stalling of the droplet in the channel. Several electrode configurations were investigated for application purposes. Using pattern electrodes on both sides of the channel can lead to a greater peak in force, but with the caveat that net force tends to zero when the droplet interface is not near the electrode edges. The continuous transport of a droplet using pattern electrodes has also been demonstrated.

### Acknowledgments

The authors would like to acknowledge funding from the Air Force Office of Scientific Research (AFOSR) and the National Science Foundation (NSF). The authors benefited from discussions with Mr. E. Baird.

### Conflicts of Interest

The authors declare no conflicts of interest.

## References

1. Pollack, M., R. Fair & A. Shenderov. 2000. Electrowetting-based actuation of liquid droplets for microfluidic applications. *Appl. Phys. Lett.* **77:** 1725–1726.
2. Pollack, M., A. Shenderov & R. Fair. 2002. Electrowetting-based actuation of droplets for integrated microfluidics. *Lab Chip* **2:** 96–101.
3. Cooney, C., C.-Y. Chen, A. Nadim & J. Sterling. 2006. Electrowetting droplet microfluidics on a single planar surface. *Microfluid Nanofluid* **2:** 435–446.
4. Cho, S., H. Moon & C. Kim. 2003. Creating, transporting, cutting, and merging liquid droplets by electrowetting-based actuation for digital microfluidic circuits. *IEEE J. MEMS* **12:** 70–80.
5. Lee, J., H. Moon, J. Fowler, *et al*. 2001. Addressable micro liquid handling by electric control of surface tension. In *Proc. IEEE Int. Conf. MEMS*, pp. 499–502.
6. Wang, K. & T. Jones. 2005. Electrowetting dynamics of microfluidic actuation. *Langmuir* **21:** 4211–4217.
7. Shapiro, B., H. Moon, R. Garrell & C. Kim. 2003. Equilibrium behavior of sessile drops under surface tension, applied external fields, and material variations. *J. Appl. Phys.* **93:** 5794–5811.
8. Charkrabarty, K. & J. Zeng. 2006. *Design Automation Methods and Tools for Microfluidics-Based Biochips*. Springer. Dordrecht, the Netherlands.
9. Mohseni, K. 2005. Effective cooling of integrated circuits using liquid alloy electrowetting. In *Proceedings of the Semiconductor Thermal Measurement, Modeling, and Management Symposium (SEMI-Therm), IEEE*.
10. Mohseni, K. & E. Baird. 2007. Digitized heat transfer using electrowetting on dielectric. *Nanoscale Microscale Thermophys. Eng.* **11:** 99–108.

11. Baird, E. & K. Mohseni. 2007. Digitized heat transfer: a new paradigm for thermal management of compact micro-systems. IEEE Transactions on Components and Packaging Technologies.
12. Mohseni, K. & A. Dolatabadi. 2006. An electrowetting microvalve: numerical simulation. *Ann. N. Y. Acad. Sci.* **1077:** 415–425.
13. Dolatabadi, A., K. Mohseni & A. Arzpeyma. 2006. Behaviour of a moving droplet under electrowetting actuation: Numerical simulation. *Can. J. Chem. Eng.* **84:** 17–21.
14. Chang, Y.-J., K. Mohseni & V. Bright. 2007. Fabrication of tapered SU-8 structure and effect of sidewall angle for a variable focus microlens using EWOD. *Sens. Actuat. A* **136:** 546–553.
15. Cho, S., S. Fan, H. Moon & C. Kim. 2002. Towards digital microfluidic circuits: creating, transporting, cutting, and merging liquid droplets by electrowetting-based actuation. In *Technical Digest. MEMS, Proc. 15th IEEE Int. Conf. MEMS*, pp. 32–35.
16. Moon, H., S. Cho, R. Garrell & C. Kim. 2002. Low voltage electrowetting-on-dielectric. *J. Appl. Phys.* **92:** 4080–4087.
17. Fair, R., V. Srinivasan, H. Ren, *et al*. 2003. Electrowetting-based on-chip sample processing for integrated microfluidics. In *IEEE Inter. electron devices meeting (IEDM)*.
18. Gascoyne, P., J. Vykoukal, J. Schwartz, *et al*. 2004. Dielectrophoresis-based programmable fluidic processors. *Lab Chip* **4:** 299–309.
19. Deval, J., P. Tabeling & C. Ho. 2002. A dielectrophoretic chaotic mixer. In *Technical Digest (ISBN-0-7803-7187-9), of the 15th IEEE International Conference on MEMS (MEMS 2002)*, pp. 36–39.
20. Jones, T. 2002. On the relationship of dielectrophoresis and electrowetting. *Langmuir* **18:** 4437–4443.
21. Jones, T., J. Fowler, Y. Chang & C. Kim. 2003. Frequency-based relationship of electrowetting and dielectrophoretic liquid microactuation. *Langmuir* **19:** 7646–7651.
22. Jones, T. & K. Wang. 2004. Frequency-dependent electromechanics of aqueous liquids: electrowetting and dielectrophoresis. *Langmuir* **20:** 2813–2818.
23. Jackson, J. 1998. *Classical Electrodynamics*. Wiley & Sons. New York.
24. Landau, L., E. Lifshitz & L. Pitaevskii. 1984. *Electrodynamics of Continuous Media*,Vol. 8, 2nd ed. Pergamon Press. New York.
25. Saville, D. 1997. Electrohydrodynamics: the Taylor-Melcher leaky-dielectric model. *Annu. Rev. Fluid Mech.* **29:** 27–64.
26. Singh, P. & N. Aubry. 2007. Transport and deformation of droplets in a microdevice using dielectrophoresis. *Electrophoresis* **28:** 644–657.
27. Walker, S. & B. Shapiro. 2006. Modeling the fluid dynamics of electrowetting on dielectric (EWOD). *IEEE J. MEMS* **15:** 986–1000.
28. Baird, E., P. Young & K. Mohseni. 2007. Electrostatic force calculation for an ewod-actuated droplet. *Microfluid Nanofluid* **3:** 635–644.
29. Young, P. & K. Mohseni. 2008. Calculation of DEP and EWOD forces for application in digital microfluidics. *ASME J. Fluids Eng*. **130**(8): 2008 (9 pp).
30. Stratton, J. 1941. *Electromagnetic Theory*. McGraw-Hill Book Company. New York.
31. Penfield, P. & H. Haus. 1967. *Electrodynamics of Moving Media*. MIT Press. Cambridge, MA.
32. Woodson, H. & J. Melcher. 1968. *Electromechanical Dynamics, Part I: Discrete Systems*. John Wiley & Sons. New York.
33. Bobbio, S. 2000. *Electrodynamics of Materials: Forces, Stresses, and Energies in Solids and Fluids*. Academic Press New York.
34. Melcher, J. 1981. *Continuum Mechanics*. MIT Press. Cambridge, MA.
35. Baird, E., P. Young & K. Mohseni. 2007. Electrostatic force calculation for an ewod-actuated droplet. *Microfluid Nanofluid* **3:** 635–644.
36. Mohseni, K. & E. Baird. 2007. A unified velocity model for digital microfluidics. *Nanoscale Microscale Thermophys. Eng.* **11:** 109–120.
37. Liu, X., R. Fedkiw & M. Kang. 2000. A boundary condition capturing method for poisson's equation on irregular domains. *J. Comput. Phys.* **160:** 151–178.